Acta Biomaterialia 28 (2015) 121–127

Contents lists available at ScienceDirect

Acta Biomaterialia

journal homepage: www.elsevier.com/locate/actabiomat

Highly selective BSA imprinted polyacrylamide hydrogels facilitated by a metal-coding MIP approach

H.F. EL-Sharif [a], H. Yapati [b], S. Kalluru [b], S.M. Reddy [a,*]

[a] Department of Chemistry, FEPS, University of Surrey, Guildford, United Kingdom
[b] Department of Chemistry, Sri Venkateswara University, Tirupati, India

ARTICLE INFO

Article history:
Received 9 April 2015
Received in revised form 24 July 2015
Accepted 8 September 2015
Available online 9 September 2015

Keywords:
Smart materials
Molecularly imprinted polymers (MIPs)
Proteins
Metal ion coordination
Selectivity

ABSTRACT

We report the fabrication of metal-coded molecularly imprinted polymers (MIPs) using hydrogel-based protein imprinting techniques. A Co(II) complex was prepared using (E)-2-((2 hydrazide-(4-vinylbenzyl) hydrazono)methyl)phenol; along with iron(III) chloroprotoporphyrin (Hemin), vinylferrocene (VFc), zinc (II) protoporphyrin (ZnPP) and protoporphyrin (PP), these complexes were introduced into the MIPs as co-monomers for metal-coding of non-metalloprotein imprints. Results indicate a 66% enhancement for bovine serum albumin (BSA) protein binding capacities (*Q*, mg/g) via metal-ion/ligand exchange properties within the metal-coded MIPs. Specifically, Co(II)-complex-based MIPs exhibited 92 ± 1% specific binding with Q values of 5.7 ± 0.45 mg BSA/g polymer and imprinting factors (IF) of 14.8 ± 1.9 (MIP/non-imprinted (NIP) control). The selectivity of our Co(II)-coded BSA MIPs were also tested using bovine haemoglobin (BHb), lysozyme (Lyz), and trypsin (Tryp). By evaluating imprinting factors (*K*), each of the latter proteins was found to have lower affinities in comparison to cognate BSA template. The hydrogels were further characterised by thermal analysis and differential scanning calorimetry (DSC) to assess optimum polymer composition.

Statement of significance

The development of hydrogel-based molecularly imprinted polymer (HydroMIPs) technology for the memory imprinting of proteins and for protein biosensor development presents many possibilities, including uses in bio-sample clean-up or selective extraction, replacement of biological antibodies in immunoassays and biosensors for medicine and the environment. Biosensors for proteins and viruses are currently expensive to develop because they require the use of expensive antibodies. Because of their biomimicry capabilities (and their potential to act as synthetic antibodies), HydroMIPs potentially offer a route to the development of new low-cost biosensors.
Herein, a metal ion-mediated imprinting approach was employed to metal-code our hydrogel-based MIPs for the selective recognition of bovine serum albumin (BSA). Specifically, Co(II)-complex based MIPs exhibited a 66% enhancement (in comparison to our normal MIPs) exhibiting 92 ± 1% specific binding with *Q* values of 5.7 ± 0.45 mg BSA/g polymer and imprinting factors (IF) of 14.8 ± 1.9 (MIP/non-imprinted (NIP) control).
The proposed metal-coded MIPs for protein recognition are intended to lead to unprecedented improvement in MIP selectivity and for future biosensor development that rely on an electrochemical redox processes.

1. Introduction

Reports of molecularly imprinted polymers (MIPs) as promising vehicles for specific molecular recognition has risen exponentially over the past 20 years [1–8]. Undoubtedly, these smart polymers will find numerous applications in drug delivery, controlled release and monitoring of drug and metabolite concentrations [9–12]. However, there is still currently a bottle-neck in translating MIP research into high impact biological applications. The problem lies in the fact that currently MIPs as synthetic antibodies still cannot compete with their biological counterparts [10].

* Corresponding author.
E-mail address: s.reddy@surrey.ac.uk (S.M. Reddy).

http://dx.doi.org/10.1016/j.actbio.2015.09.012
1742-7061/

Molecular imprinting can generally be achieved through a number of synthetic strategies (e.g. covalent, non-covalent, semi-covalent and metal ion-mediated imprinting) depending on the types of interactions desired, as described in Fig. 1. Of these approaches, metal ion-mediated imprinting is of great interest to introduce enhanced functionality into recognition sites of MIPs; depending on the metal, its oxidation state and ligand characteristics, the strength of interaction can vary enormously [2,13]. Metal ions are known to bind functional groups through the sharing of electrons from the atoms of templates to the unfilled orbitals of the outer coordination sphere of the metal [2,13–17]. For example, Sreenivasan illustrated the possibility of improving imprinting efficiencies of polyaromatic hydrocarbons (PAHs), namely naphthalene, by pre-associating a metal ion prior to polymerisation of poly(2-hydroxyethyl methacrylate) (pHEMA) hydrogels [14]. It was proposed that due to the lack of functional groups (e.g. OH, COOH, NH_2, etc.), inadequate and inefficient affinity sites would hinder MIP functionality for such PAH molecules. In turn, the addition of metal ions to pHEMA, such as silver (Ag^+), could impart enhanced interactions between the functional monomers and the PAHs. As a result of incorporating Ag^+ ions during the synthesis (in the form of silver nitrate), the equilibrium uptake of the template naphthalene molecule rose from 3.3 ± 0.4 mg/100 mg (without using Ag ions) to 66.0 ± 2 mg/100 mg, resulting in an impressive MIP to NIP imprinting factor of 27.5:1. Therefore, it appeared that the adsorption capacity of molecules lacking essential anchoring functional groups can be increased by inclusion of metal ions [14]. Consequently, metal coordination has been employed in MIPs for small organic molecule recognition as an alternative means of association between template and functional monomer [2]. This approach was first reported by Fujii et al. for the imprinting of chiral amino acids [18]. In this approach, metal complexes generally consisted of polymerizable ligand(s) to complex the metal ion (typically a transition metal ion) which in turn coordinated to the template. As such, metalloporphyrins have been widely explored for small molecule imprints and researchers have hypothesised that three-dimensional binding sites occurred on the porphyrin plane via metal coordination ultimately leading to co-operative contribution to specific binding [15–19].

Herein, we investigate the feasibility of fabricating metal-coded MIPs for biomacromolecule recognition (namely, proteins), within polyacrylamide hydrogels. A chelating Co(II) complex was synthesised using a (E)-2-((2 hydrazide-(4-vinylbenzyl)hydrazono) methyl)phenol ligand comprising bifunctional vinyl groups purposefully chosen for co-polymerisation within the polyacrylamide matrix. Cobalt (Co) is one of the essential trace elements and plays a number of crucial roles in many biological functions such as in vitamin B12 for formation of red blood corpuscles, and in nitrogen fixation by microorganisms in plants [20–22]. Hydrazones are also an important class of Schiff base compounds possessing pharmacological applications as antimicrobial, anti-inflammatory, and anti-tumoral agents [20]. Hydrazone compounds also display versatile behaviours in metal coordination and their biological activity is often increased by bonding to transition metals. One example is the biological activity of d-metal complexes of N-heteroaromatic hydrazones of 2-pyridinecarboxaldehyde which is often higher in comparison to the corresponding free ligand [20–22].

Iron(III) chloroprotoporphyrin (Hemin), vinylferrocene (VFc), zinc(II) protoporphyrin (ZnPP), and protoporphyrin (PP) were also investigated as additional functional group co-monomers for enhanced template association and for their electrochemical activity. These complexes were chosen on the basis that metal ions in metalloporphyrin-based receptors can serve as Lewis acid sites to bind Lewis bases such as amines [15]. Thus, metalloporphyrin inclusion in hydrogel MIP systems would create additional interactions for template protein molecules, and ultimately could provide an essential redox centre in the development of electrochemical biosensors [23–30]. In this paper, the latter complexes were introduced into the MIPs as co-monomers (and/or cross-linkers) for metal-coding of the imprinted cavities for the selective recognition

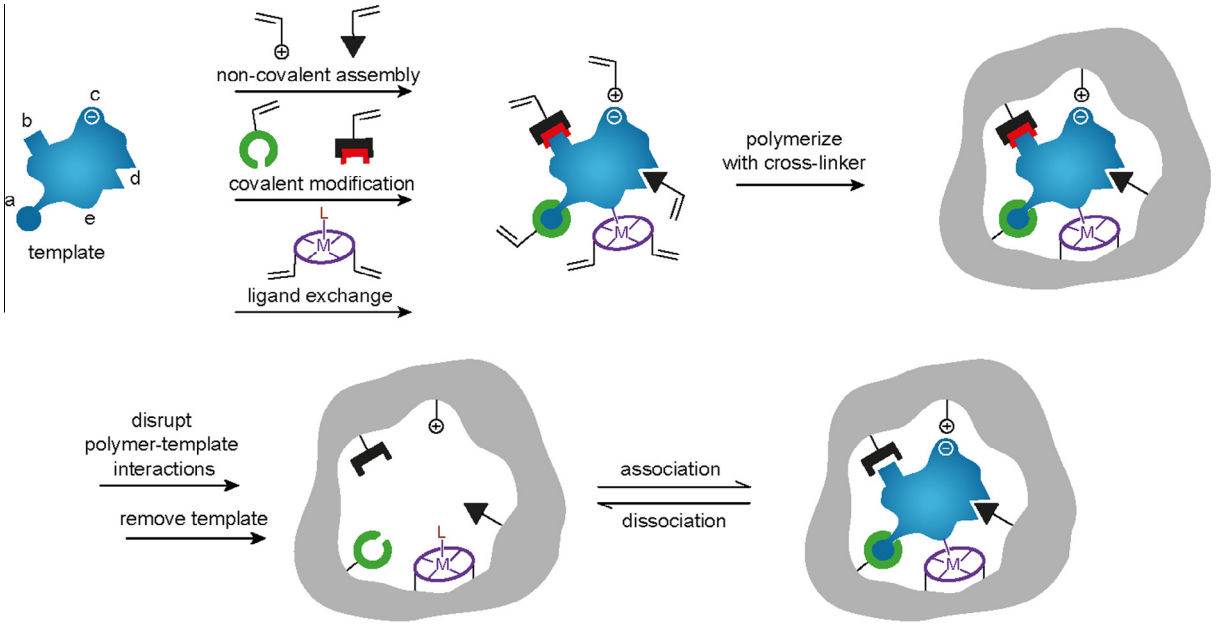

Fig. 1. Schematic representation of the imprinting process illustrating the reversible interactions between template and polymerizable functional monomers used in creating affinity. Depending on the synthetic strategy this may involve one or more of the following interactions: (a) reversible covalent bonds, (b) covalently attached polymerizable binding groups that are activated for non-covalent interaction by template cleavage (sacrificial spacer or semi-covalent strategy), (c) electrostatic interactions, (d) hydrophobic or van der Waals interactions, (e) co-ordination with a metal centre. Each, (a–e) respectively are formed with complementary functional groups or structural elements of the template. Subsequent polymerisation in the presence of a cross-linker produces a porous matrix in which template sites are located; these can then be removed through disruption of polymer–template interactions (a–e), and extracted from the matrix. Template(s), or analogues thereof, may then be selectively rebound by the polymer in the sites/cavities vacated by template, or the imprints. Reproduced with permission from Ref. [2].

of the non-metallo proteins bovine serum albumin (BSA). The proposed metal-coded MIPs for protein recognition are intended to lead to unprecedented improvement in MIP selectivity and for future biosensor development that rely on electrochemical redox processes.

2. Experimental section

2.1. Reagents

Acrylamide (AA), *N*,*N*-methylenebisacrylamide (bis-AA), ammonium persulphate (APS), *N*,*N*,*N*,*N*-tetramethylethylenediamine (TEMED), sodium dodecyl-sulphate (SDS), glacial acetic acid (AcOH), tris(hydroxymethyl)-amine (Tris-base), tris (hydroxymethyl)-amine hydrochloride (Tris–HCl), dimethylformamide (DMF), dimethyle solfoxide (DMSO), 4-vinylbenzyl chloride, 2-hydroxybenzaldehyde, hydrazine hydrate, cobalt chloride, iron(III) chloroprotoporphyrin IX (Hemin), vinylferrocene (VFc), zinc(II) protoporphyrin IX (ZnPP), protoporphyrin IX (PP), haemoglobin (bovine, H 2500, BHb), serum albumin (bovine, A3059, BSA), Lysozyme (hen egg white, L7651), Trypsin (bovine pancreatic, T4665) were all purchased from Sigma–Aldrich, Poole, Dorset, UK. Sieves (75 μm) were purchased from Inoxia Ltd., UK.

2.2. Synthesis of ligand

A Schiff base ligand of (E)-2-((2 hydrazide-(4-vinylbenzyl)hydra zono)methyl)phenol was prepared by mixing a solution of 4-vinylbenzyl chloride (5 mL, 0.03 mol) in absolute ethanol (12.5 mL) along with hydrazine hydrate (1.5 mL, 0.03 mol) under continuous stirring, the resulting mixture was refluxed on a water bath for 4 h. After completion of the reaction, the mixture was cooled at room temperature and a white precipitate of hydrazide was filtered and collected. The resulting hydrazide (2 g, 0.013 mol) was then dissolved and stirred in ethanol (10 mL) with an equivalent amount of 2-hydroxybenzaldehyde (1.37 mL, 0.013 mol). To this, a catalytic amount of glacial acetic acid was added, and the reaction mixture was heated to 70–80 °C for 4–6 h. The completion of the reaction was noted by the formation of the ligand as a yellow solid. The ligand was monitored by thin-layer chromatography (TLC) and then separated by filtration and recrystallized. Yield: 80%, MP: 164–166 °C, Elemental analysis, found (calcd.) for $C_{16}H_{16}N_2O$: C, 76.16 (76.01); H, 6.39 (6.44); N, 11.10 (11.05); O, 6.34 (6.42)%. IR data (KBr, cm^{-1}); 3384 ν(NH), 1602 ν(C═N), 3419 ν(O—H). ^1H NMR (DMSO-d_6): δ 11.26 (s, 1H, OH), 2.34 (1H, s, NH), 8.54 (1H, s, —N═CH), 7.02–7.66 (8H, m, Aromatic) 3.91 (2H, d, CH_2) 6.63 (1H, s, CH), 5.18 (2H, d, CH_2). ^{13}C NMR (DMSO-d6) in δ (ppm): 143.3 (C═N), 56.0 (CH_2), 136.10 (CH), 114.3 (═CH_2), 117.8–157.2 (Aromatic carbons).

2.3. Synthesis of Co(II) complex

The bifunctional vinyl Co(II) complex was prepared by addition of the (E)-2-((2 hydrazide-(4-vinylbenzyl)hydrazono)methyl)phe nol ligand (2 mmol) along with cobalt chloride (1 mmol) to a hot solution (60 °C) of ethanol and water (1:1, 25 mL). The resulting mixture was then stirred under reflux for 1–2 h. The completion of the reaction was noted by the formation of a reddish brown solid. The precipitate was filtered and washed twice with a 1:1 ethanol: water mixture. Yield: 82%. MP: 320–323 °C, Anal. calcd. For $C_{32}H_{30}CoN_4O_2$: C, 68.44 (68.22); H, 5.38 (5.29); N, 9.98 (10.06); O, 5.70 (5.66); Co, 10.49 (10.58)%. IR data (KBr, cm^{-1}); 3375 ν(NH), 1586 ν(C═N). Electronic spectra (DMF, cm^{-1}); 21,768 and 27,735 cm^{-1}.

Characterisation of both the (E)-2-((2 hydrazide-(4-vinylben zyl)hydrazono)methyl)phenol ligand and Co(II) complex were performed by elemental analysis, FT-IR, 1H NMR, electronic spectra.

2.4. MIP preparation

Hydrogel-based MIPs (HydroMIPs) were synthesised using 0.76 M of AA monomer (54 mg) along with 38.92 mM (6 mg) of bis-AA as cross-linker for each hydrogel. Template protein (BSA, 66 kDa; 12 mg, 181.8 μM) was also added followed by initiator (20 μL of a 10% (w/v) APS solution, 8.77 mM) and catalyst (20 μL of a 5% (v/v) TEMED solution, 8.61 mM) along with 50 mM Tris buffer pH 7.4 to give final volumes of 1 mL. For the imprinting of metal-coded MIPs, appropriate amounts of complexes Hemin, VFc, ZnPP, PP or Co-complex (dissolved in DMF) were also added to give a final concentration of 0.2 mM. Solutions were purged with nitrogen for 5 min and polymerisation occurred overnight at room temperature (~22 °C), giving final total gel densities (%T) of 6%T, AA/bis-AA (w/v) and final crosslinking densities (%C) of 10%C (9:1, w/w) for all hydrogels. Molar ratios of monomer and cross-linker to template protein were at 4180:1 and 214:1, respectively. For every MIP hydrogel created a non-imprinted control polymer (NIP) was prepared in an identical manner but in the absence of template protein. Both HydroMIPs and NIPs are semi-translucent and have a gel-like appearance and texture that vary based on functional monomer/co-monomer, and %T gel composition.

After polymerisation, the gels were granulated separately using a 75 μm sieve. Of the resulting gels, 500 mg were washed with five 1 mL volumes of 50 mM Tris buffer pH 7.4 followed by five 1 mL volumes of 10% (w/v):10% (v/v) SDS:AcOH (pH 2.8) and another five 1 mL volume washes of MilliQ water to remove any residual 10% (w/v):10% (v/v) SDS:AcOH eluent followed by a further wash of 50 mM Tris buffer pH 7.4 to equilibrated the gels. Each wash step was followed by a centrifugation, whereby the gels were vortexed then centrifuged using an Eppendorf mini-spin plus centrifuge for 3 min at 6000 rpm (RCF: 2419*g*). All supernatants were collected for spectrophotometry analysis to verify the extent of template removal. It should be noted that the last water wash and SDS:AcOH eluent fractions were not observed to contain any protein. Therefore, we are confident that any remaining template protein within the MIPs did not continue to leach out during future studies.

2.5. MIP characterisation

2.5.1. Spectrophotometric analysis

The subsequent rebinding effect of the conditioned and equilibrated MIPs and NIPs were characterised using a UV mini-1240 CE spectrophotometer (Shimadzu Europa, Milton Keynes, UK). Hydrogels (500 mg) were then treated with 1 mL of a 3 mg mL^{-1} template protein solution of either BSA, BHb, Lyz or Tryp, and polymer/protein solutions were mixed on a rotary vortex mixer then allowed to associate at room temperature (~22 °C) for 20 min followed by centrifugation. The hydrogels were then washed four times with 1 mL MilliQ water. Each reload and wash step for the hydrogels was followed by centrifugation at 6000 rpm (RCF: 2419*g*) for 3 min. All supernatants were collected for analysis by spectrophotometry (at 404 nm for BHb and 280 nm for BSA, Lyz and Tryp).

2.5.2. Thermal analysis

Thermal stability and the glass transition temperature (T_g) of the polymer materials were determined using both thermogravimetric analysis (TGA) and differential scanning calorimetry

(DSC). TGA was performed by a TGA Q500 V6.7 Build 203 (Universal V4.7A TA Instruments, UK) under nitrogen atmosphere from 25 to 600 °C at a heating rate of 10 °C/min. DSC was performed using a DSC Q1000 V9.9 Build 303 (Universal V4.7A TA Instruments, UK) using a heat/cool/heat test method (rate of 10 °C/min) to eliminate the effect of moisture [31]. DSC thermograms of each sample were obtained from the second heating run (from 0 to 250 °C) after a first heating run from 0 to 150 °C, and T_g values were taken as the midpoint of transition (half height). All TGA/DSC measurements were performed using 5–10 mg of dried samples under an atmosphere of nitrogen gas.

2.6. Statistical evaluation

Percentage specific binding was calculated using the amount of MIP protein binding subtracted from that binding in NIP; this value is then divided by the initial protein loaded concentration, i.e. $[C_i - C_r]_{MIP} - [C_i - C_r]_{NIP}/C_i$, where C_i and C_r are the initial protein and the recovered protein concentrations (mg/mL) respectively. Significance ($^{*}P < 0.05$, $^{**}P < 0.01$ or $^{***}P < 0.005$) was calculated using an unpaired two-tailed Student's t-test ($n = 3$), data represents mean ± S.D., $n = 3$.

3. Results and discussion

3.1. Co(II) complex characterisation

It appears from the elemental analysis data that the reaction between cobalt chloride and the ligand occur in a 1:2 (metal:ligand) molar ratio. The complex is insoluble in common organic solvents viz. ethanol, methanol, chloroform, benzene, cyclohexane, acetone, diethyl ether, etc., but is soluble in DMF and DMSO. Structures of the Co-complex, along with hemin, ZnPP, PP, and VFc are illustrated in Fig. 2. It should be noted that all complexes comprise vinyl groups purposefully chosen for the ability to co-polymerise within the polyacrylamide structure and provide additional functional groups to associate with the template.

3.2. IR spectral analysis

The IR spectra of the free ligand and its corresponding Co(II) complex was compared to deduce information about the coordination behaviour of the ligand with metal (Fig. 3). The IR spectra of the (E)-2-((2 hydrazide-(4-vinylbenzyl)hydrazono)methyl)phenol displayed an absorption band at 3333 cm^{-1} due to O—H stretching. The band due to O—H stretching frequency overlaps with the band due to N—H stretching frequency. The absence of ν(OH) in its Co(II) complex, indicates deprotonation of —OH group during complexation. The ν(C=N) observed at 1610 cm^{-1} in the spectra of ligand, shifted to lower frequency (15 cm^{-1}) in its metal complex suggesting coordination of the azomethine group with metal.

3.3. ^1H NMR analysis

The formation of ligand was supported by ^1H NMR spectra, and the appearance of a sharp singlet at 2.34 ppm, corresponds to the NH proton. A singlet at 11.26 corresponds to an —OH proton. The disappearance of the phenolic —OH proton signal in the Co(II) complex indicates the bonding through a phenolate-oxygen with metal. The multi signals within the range of 7.02–7.66 ppm are assigned to the aromatic protons. These signals are shifted towards low field in the metal complexes. This information suggests the adjustment of electronic current upon coordination of ⩾C=N group to the metal ion.

3.4. Electronic spectrum

The electronic spectrum of the ligand exhibited absorption bands at 47,619 cm^{-1} and 37,735 cm^{-1} corresponding to π–π* transitions of the aromatic system. The broad band at 26,667 cm^{-1} is due to the transition within the molecule, essentially an intra-molecular charge transfer interaction. The electronic spectrum of Co(II) complex showed two spin-allowed transitions at 21,768 and 27,735 cm^{-1}, these bands correspond to $^2B_{2g} \rightarrow {}^2E_g$ and $^2B_{2g} \rightarrow {}^2A_{1g}$ transitions respectively. The positions of the bands indicate that the Co(II) complex has four coordinated square planar geometry [20].

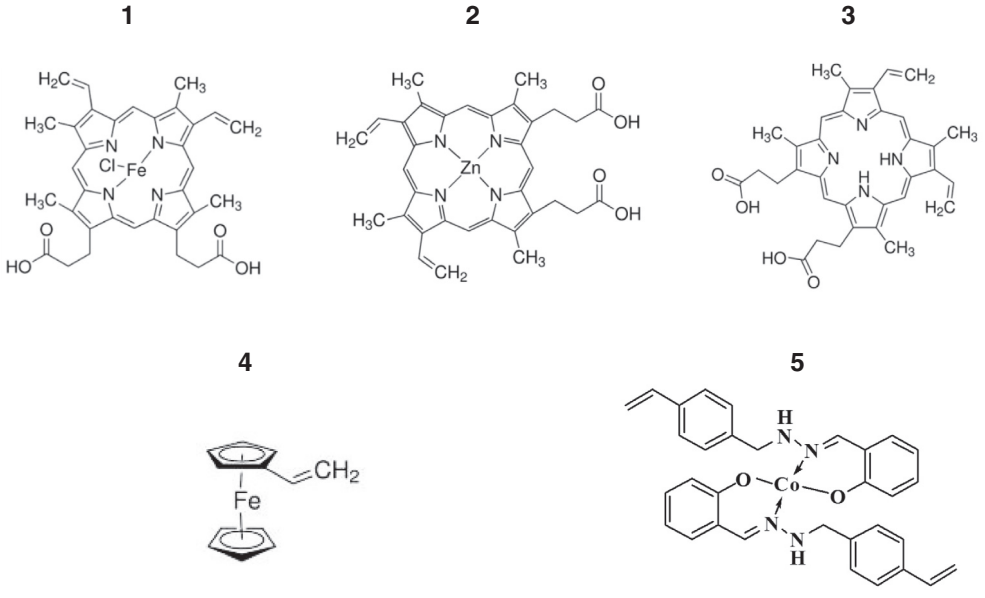

Fig. 2. Metal complex structures; 1 iron(III) chloroprotoporphyrin IX (Hemin), 2 zinc(II) protoporphyrin IX (ZnPP), 3 protoporphyrin IX (PP), 4 vinylferrocene (VFc), 5 Co(II) complex (illustrating the (E)-2-((2 hydrazide-(4-vinylbenzyl)hydrazono)methyl)phenol ligand attachment via two nitrogens).

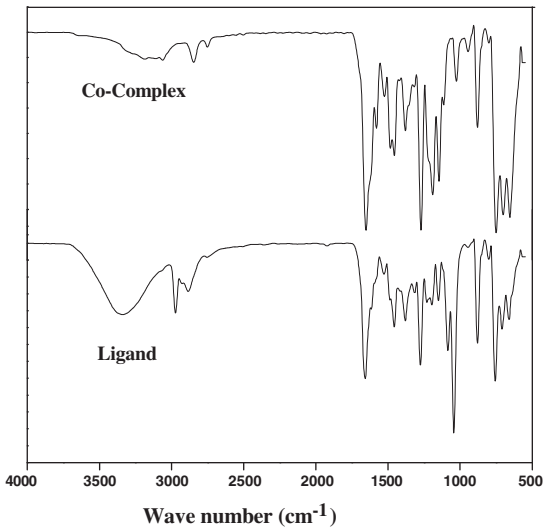

Fig. 3. FT-IR spectrum of the (E)-2-((2 hydrazide-(4-vinylbenzyl)hydrazono) methyl)phenol ligand and Co(II) complex.

3.5. MIP characterisation

The molecular imprinting effect was characterised by calculating the rebinding capacity (Q) of protein to the gel polymer (mg g^{-1}) exhibited by the protein-specific MIP and the control NIP using Eq. (1), where C_i and C_r are the initial protein and the recovered protein concentrations (mg/mL) respectively (which specifies the specific protein bound within the gel), V is the volume of the initial solution (mL), and g is the mass of the gel polymers (g).

$$Q = [C_i - C_r]\,V/g \quad (1)$$

The imprinting factor (IF), sometimes referred to as the selectivity ratio (α) is expressed either by assessing the specific binding in the MIP per binding in NIP i.e. $[C_i - C_r]_{MIP}/[C_i - C_r]_{NIP}$, or simply by comparing the latter calculated binding capacities (Q) for MIP and NIP, as in Eq. (2):

$$IF = Q_{MIP}/Q_{NIP} \quad (2)$$

Table 1 illustrates the rebinding capacities (Q) and imprinting factors (IF) of BSA using different MIP compositions at optimum metal complex concentrations. Our standard MIPs (i.e. MIPs without metal) exhibited the lowest Q values of 3.2 ± 0.52 mg g^{-1} (IF = 1.8 ± 0.27), whereas highest Q values of 5.7 ± 0.45 mg g^{-1} and IF values of 14.8 ± 1.9 were exhibited by Co(II)-coded MIPs closely followed by VFc-coded MIPs (Q = 5.1 ± 0.36 mg g^{-1}, IF = 8.4 ± 1.2). Therefore, it is evident that the best imprinting effects of BSA rely on the presence of metal-ion centre within metal-coded MIPs. Protoporphyrin IX contains a tetrapyrrole ring structure, and could contribute to the MIP cavity by forming π–π stacking interactions with any number of exposed aromatic amino-acids such as histidine or proline. VFc also has an aromatic ring that can form similar interactions. Both the zinc(II) and iron (II)/(III) in the ZnPP, VFc and Hemin structures could further coordinate with BSA to form more specific recognition sites in the MIP polymer matrix. The same is true for the Co-complex, where the Co (II) is also able to coordinate its metal ion within the MIP matrix and can bind functional groups through the donation of electrons from the atoms of templates to the unfilled orbitals of the outer coordination sphere of the metal. It was not possible to compare the functionality of the (E)-2-((2 hydrazide-(4-vinylbenzyl)hydra zono)methyl)phenol ligand in the MIP matrix with its counterpart Co(II) complex due to a lack of solubility in the polymerisation stage. The immiscibility of the ligand ultimately lead to precipitation of BSA protein in the organic phase and inhibited the production of MIP polymers. Thus, from the enhanced affinities, it is plausible that the coordination metal ion electron acceptors along with π backbonding can complex with many of the protein backbone amino acid chains electron donors and numerous favourable interactions occur by weak charge transfer interactions within these polyacrylamide-based MIPs. This in turn can lead to a more stable conformational compatibility between the protein template and the MIP cavity region.

Table 1
Comparison of the different polyacrylamide hydrogel MIP compositions on the rebinding capacities (Q, mg BSA/g polymer) imprinting factors (IF), and percentage specific binding of BSA. Data represents mean ± S.D., n = 3, % error also included.

Polymer	Binding capacity Q (mg/g)	Imprinting factor IF	% [Specific binding]
MIP	3.2 ± 0.52 (±16%)	1.8 ± 0.27 (±15%)	26 ± 6%
NIP	1.8 ± 0.52 (±27%)		
MIP_{PP}	4.2 ± 0.61 (±15%)	1.9 ± 0.16 (±8%)	34 ± 5%
NIP_{PP}	2.1 ± 0.30 (±14%)		
MIP_{Hemin}	3.4 ± 0.12 (±4%)	2.4 ± 0.11 (±5%)	34 ± 1%
NIP_{Hemin}	1.4 ± 0.07 (±5%)		
MIP_{ZnPP}	4.7 ± 0.24 (±5%)	2.4 ± 0.64 (±27%)	48 ± 14%
NIP_{ZnPP}	1.9 ± 0.39 (±20%)		
MIP_{VFc}	5.2 ± 0.36 (±7%)	8.4 ± 1.2 (±14%)	79 ± 2%
NIP_{VFc}	0.6 ± 0.14 (±22%)		
$MIP_{Co\text{-}complex}$	5.7 ± 0.45 (±8%)	14.9 ± 1.9 (±13%)	92 ± 1%
$NIP_{Co\text{-}complex}$	0.4 ± 0.64 (±17%)		

The nature and volume of the solvent/porogen also play an important role in the generally accepted two stage molecular imprinting process; firstly by single phasing the polymerisation components, and secondly to regulate the macroporosity [32]. The hydrogel systems listed herein have roughly a 93% water composition. Water is a polar protic solvent with a low dipole moment (1.85 D). However, the incorporation of a small amount of an organic solvent (DMF) is reported here. DMF is a polar aprotic solvent with a high dipole moment (3.82 D), and could have adverse effects on the stability of the MIP in terms of BSA protein compatibility. Therefore, control studies including appropriate amounts of DMF in the MIP preparation were conducted to ascertain any interference within the imprinting process. Results showed no significant difference between a normal MIP (Q values of 3.2 ± 0.52 mg g^{-1}) and a MIP prepared in the presence of DMF (Q values of 3.1 ± 0.15 mg g^{-1}). The pH value of the adsorption solution plays an important role in the rebinding and selecting processes, and therefore a 50 mM Tris buffer pH 7.4 was selected for optimum rebinding [33].

Selectivity studies were also conducted to confirm the specificity of the imprinting effect by assessing the relative imprinting factor of cross-selective binding proteins. The cross-reactivity of the BSA-imprinted MIPs for non-cognate proteins was quantified using relative imprinting factors (K), Eq. (3), where $IF_{template}$ is the imprinting factor for the original template, and $IF_{analogue}$ is the imprinting factor of the analogue proteins. For the template BSA K = 1, and for the non-cognate proteins that are less-specific for the BSA MIP, K < 1.

$$K = IF_{analogue}/IF_{template} \quad (3)$$

Therefore, based on the best imprinting effect exhibited by the Co(II)-coded MIP, the cross-selectivity was also tested using bovine haemoglobin (BHb), lysozyme (Lyz), and trypsin (Tryp). Fig. 4 illustrates the relative IF (K) for each of the latter proteins towards a BSA MIP. In terms of molecular weight, the closest resemblance to BSA, is BHb; (BSA MW: 67.0 kDa, isoelectric point (pI) 4.8; BHb MW: 64.5 kDa, pI 6.8; Lyz MW: 14.4 kDa, pI 11.2; Tryp MW: 23.8 kDa, pI 9.3). It can be seen from the data that for a BSA–MIP,

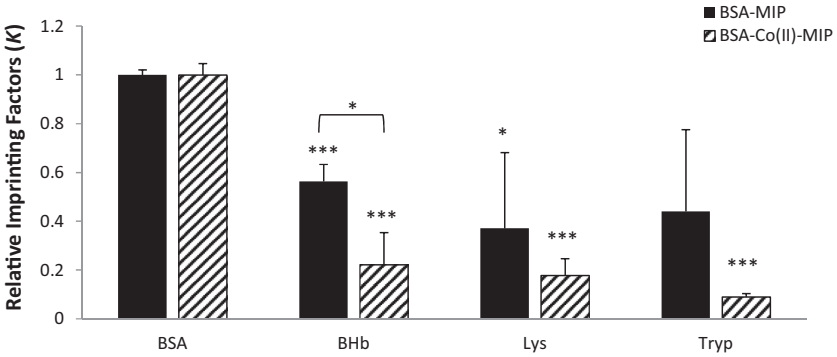

Fig. 4. Relative imprinting factors (K) for a BSA–MIP and a metal-coded BSA–MIP using Co(II) complex. Results illustrate higher MIP selectivities for template BSA in comparison to non-template analytes with significantly lower K values when using a Co(II)–MIP. Significance ($^{*}P < 0.05$, $^{**}P < 0.01$ or $^{***}P < 0.005$) was calculated using an unpaired two-tailed Student's t-test ($n = 3$), error bars represent S.D.

BHb exhibits the closest selectivity to BSA ($K = 0.56 \pm 0.07$). Since the diameter of BHb and BSA are approximately 5.5 nm and 15.5 nm respectively, recognition is unlikely to be based on protein dimensional size. Based on their molecular weight similarity, the molar ratio of monomer:protein (4180:1) will be similar for both BHb and BSA. Therefore, we would expect a similar number of monomer molecules to interact with each protein molecule during cavity formation. When incorporating 0.2 mM of a di-vinyl functionalised metal complex into the polymerising matrix (to produce Co(II)-coded MIP), the Co-complex can act as an additional cross-linker during the polymerisation and so theoretically, it will also be present at the cavity albeit at a much smaller molar concentration (0.5%) compared with the main cross-linking agent, bis-acrylamide. Interestingly, in the presence of this Co-complex bound MIP, the cross-selectivity of the BSA–Co(II)–MIP towards BHb is reduced by a factor of 2.5 ($K = 0.22 \pm 0.13$). It seems that the metal-complex modified MIP matrix is capable of forming more stable and importantly, a highly selective protein-polymer complex for the cognate protein BSA. Li et al. [33] have studied metal ion mediated enhancement of imprinting factor of a BSA MIP. They proposed that inclusion of a divalent ion such as Co^{2+} during polymerisation encouraged the formation of a BSA–Co(II) complex through Co interaction via both —COOH and/or N-terminus of BSA. Metal co-ordination via the protein was key to improving protein binding affinity. Our method of integrating the metal centre as part of the polymer matrix offers the advantage of interrogating selective protein binding directly without the need for initial pre-treatment of the protein or MIP with a metal ion.

Thermal analysis of the polymer composites (total monomer concentration = 6% T, w/v) using thermo-gravimetric analysis (TGA) and differential scanning calorimetry (DSC) reveal that polyacrylamide hydrogels have higher thermal degradation in the presence of a metal ligand, and thus a lower ability to preserve water (Fig. 5A). The first thermal event occurs in the temperature range 25–210 °C, where all polyacrylamide samples present a mass loss ranging from 12% to 18% due to the evaporation of water. This attribute is a function of polymer morphology and crystallinity [31]. TGA and derivative weight (%/°C) showed that both Co-complex and VFc polyacrylamide hydrogels had lower temperatures for maximum weight loss (200 °C) than pure acrylamide (210 °C). Thermal degradation of the polymer hydrogels also followed the same trend whereby polyacrylamide reached a maximum of 410 °C, with weight loss of 42% and both Co-complex and VFc polyacrylamide reached a maximum of 400 °C, with weight loss of 37% and 39% respectively.

DSC thermograms reveal that the glass-transition temperature (T_g) of pure polyacrylamide was 76.84 °C, the result comparable with previous reports of 97 °C, concentration more than 8% [31]

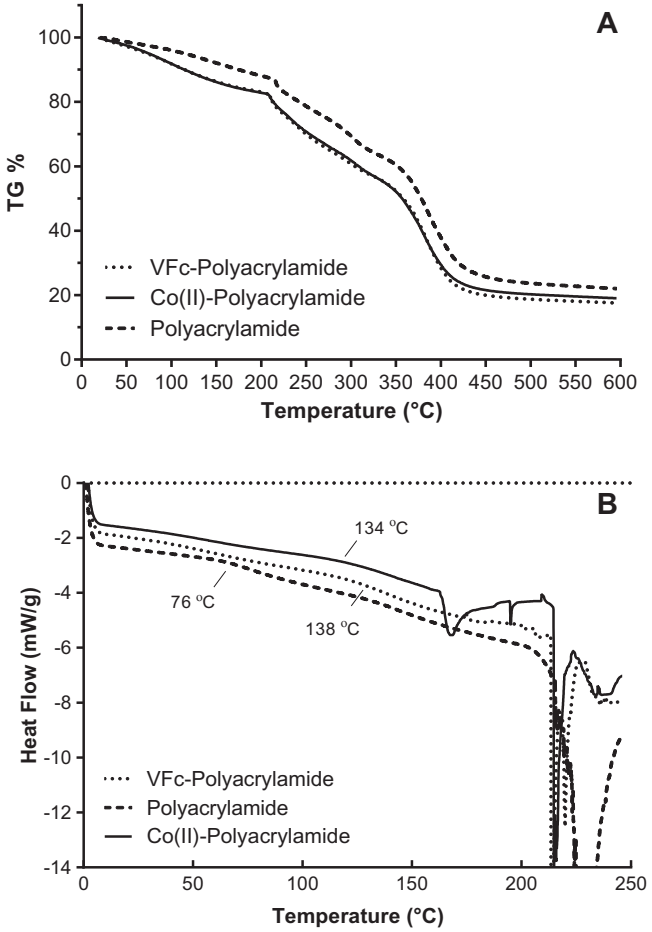

Fig. 5. Thermogravimetric analysis (TGA) curves (A), and differential scanning calorimetry (DSC) thermograms (B), for three types of hydrogels, in the absence of metal ligand (polyacrylamide), and in the presence of Co(II) complex (Co(II)-polyacrylamide), vinylferrocene (VFc-polyacrylamide).

and 70 °C, concentration less than 8% [34]. The inclusion of both Co(II) complex and VFc however result in T_g values of 134 °C and 137 °C respectively (Fig. 5B). The miscibility of polymers can be judged by the properties of the solid state such as the T_g [31]. Lower T_g values indicate a more amorphous and flexible polymer backbone, whereas higher T_g values are indicative of more crystalline structures. Most notably, addition of metal complexes resulted in T_g values of 60 °C greater than that of pure polyacrylamide, hence suggesting improved macroporosity and polymer

backbone stability. It is feasible that metal-coded MIPs can improve cavity stability via the substituted vinyl-group ligands in the complexes allowing them to act as cross-linkers and hence increasing the chain entanglement.

4. Conclusions

Iron(III) chloroprotoporphyrin (hemin), vinylferrocene (VFc), zinc(II) protoporphyrin (ZnPP) and protoporphyrin (PP), along with a bespoke cobalt Co(II) complex were introduced into hydrogel-based MIPs as co-polymers for metal-coding of a BSA protein imprint. It was concluded that metal-coded polyacrylamide MIPs exhibited higher BSA binding and selective capacities. This could be due to improved polymer backbone stability and macroporosity with T_g values of around 60 °C higher than that of pure polyacrylamide. Specifically, Co(II)-coded MIPs had the highest binding capacity (Q) values of 5.7 ± 0.45 mg BSA/g polymer and IF values of 14.8 ± 1.9. Optimum polymer compositions were further characterised by thermal analysis. Additionally, we propose that the metal itself is contributing to favourable (pi) bonding interactions with the protein. We are currently expanding this study to encapsulate other transition metal complexes in order to develop a better understanding of the metal (complex)–MIP–protein interactions leading to these optimised binding capacities. At this stage, a direct comparison of MIPs with antibodies is warranted. These metal-coded MIPs also readily lend themselves for electrochemical interrogation and hence future protein biosensor development.

Acknowledgements

The authors are grateful to Mrs Violeta Doukova for the thermo analysis (Department of Physics, University of Surrey); Dr Scott Turner for helpful discussions (Department of Chemistry, University of Surrey); DST-UKIERI (IND/CONT/R/12-13/779), and NERC/ACTF of the RSC (NE/J01/7671) for supporting this project.

References

[1] H.F. El-Sharif, Q.T. Phan, S.M. Reddy, Enhanced selectivity of hydrogel-based molecularly imprinted polymers (HydroMIPs) following buffer conditioning, Anal. Chim. Acta 809 (2014) 155–161.
[2] C. Alexander, H.S. Andersson, L.I. Andersson, R.J. Ansell, N. Kirsch, I.A. Nicholls, J. O'Mahony, et al., Molecular imprinting science and technology: a survey of the literature for the years up to and including 2003, J. Mol. Recogn. 2006 (19) (2003) 106–180.
[3] M.E. Byrne, K. Park, N.A. Peppas, Molecular imprinting within hydrogels, Adv. Drug Deliv. Rev. 54 (2002) 149–161.
[4] D.E. Hansen, Recent developments in the molecular imprinting of proteins, Biomaterials 28 (2007) 4178–4191.
[5] Y. Ge, A.P.F. Turner, Too large to fit? Recent developments in macromolecular imprinting, Trends Biotechnol. 26 (2008) 218–224.
[6] M.E. Byrne, V. Salian, Molecular imprinting within hydrogels II: progress and analysis of the field, Int. J. Pharm. 364 (2008) 188–212.
[7] S.M. Reddy, D.M. Hawkins, Q.T. Phan, D. Stevenson, K. Warriner, Protein detection using hydrogel-based molecularly imprinted polymers integrated with dual polarisation interferometry, Sensors Actuat. B: Chem. 176 (2013) 190–197.
[8] D.M. Hawkins, E.A. Ellis, D. Stevenson, A. Holzenburg, S.M. Reddy, Novel critical point drying (CPD) based preparation and transmission electron microscopy (TEM) imaging of protein specific molecularly imprinted polymers (HydroMIPs), J. Mater. Sci. 42 (2007) 9465–9468.
[9] M.P. Davies, V. De Biasi, D. Perrett, Approaches to the rational design of molecularly imprinted polymers, Anal. Chim. Acta 504 (2004) 7–14.
[10] V.J.B. Ruigrok, M. Levisson, M.H.M. Eppink, H. Smidt, J. van der Oost, Alternative affinity tools: more attractive than antibodies?, Biochem J. 436 (2011) 1–13.
[11] Y. Fuchs, X. Ton, K. Haupt, I. Dika, O. Soppera, A. Mayes, Photopolymerization and photostructuring of molecularly imprinted polymers for sensor applications, Sensors (2012) 2235–2238.
[12] S. Kunath, N. Marchyk, K. Haupt, K. Feller, Multi-objective optimization and design of experiments as tools to tailor molecularly imprinted polymers specific for glucuronic acid, Talanta 105 (2013) 211–218.
[13] A.G. Mayes, M.J. Whitcombe, Synthetic strategies for the generation of molecularly imprinted organic polymers, Adv. Drug Deliv. Rev. 57 (2005) 1742–1778.
[14] K. Sreenivasan, Improving the efficiency of imprinting in poly(HEMA) for polyaromatic hydrocarbon using silver ions, J. Appl. Polym. Sci. 109 (2008) 3275–3278.
[15] S. Chou, M. Syu, Via zinc(II) protoporphyrin to the synthesis of poly(ZnPP-MAA-EGDMA) for the imprinting and selective binding of bilirubin, Biomaterials 30 (2009) 1255–1262.
[16] M. Kempe, M. Glad, K. Mosbach, An approach towards surface imprinting using the enzyme ribonuclease A, J. Mol. Recogn. 8 (1995) 35–39.
[17] M. Kempe, K. Mosbach, Separation of amino acids, peptides and proteins on molecularly imprinted stationary phases, J. Chromatogr. 691 (1995) 317–323.
[18] Y. Fujii, K. Matsutani, K. Kikuchi, Formation of a specific co-ordination cavity for a chiral amino acid by template synthesis of a polymer Schiff base cobalt (III) complex, J. Chem. Soc. Chem. Commun. (1985) 415–417.
[19] B.R. Hart, K.J. Shea, Synthetic peptide receptors: molecularly imprinted polymers for the recognition of peptides using peptide–metal interactions, J. Am. Chem. Soc. 123 (2001) 2072–2073.
[20] Y. Harinath, D. Kumar Reddy Harikishore, B. Kumar Naresh, K. Lakshmi, K. Seshaiah, Copper(II) nickel(II) complexes of n-heteroaromatic hydrazone: synthesis, characterization and in vitro antimicrobial evaluation, J. Chem. Pharm. Res. 3 (2011) 698–706.
[21] Y. Harinath, D.H.K. Reddy, B.N. Kumar, C. Apparao, K. Seshaiah, Synthesis, spectral characterization and antioxidant activity studies of a bidentate Schiff base, 5-methyl thiophene-2-carboxaldehyde-carbohydrazone and its Cd(II), Cu(II), Ni(II) and Zn(II) complexes, Spectrochim. Acta Part A – Mol. Biomol. Spectrosc. 101 (2013) 264–272.
[22] D.H.K. Reddy, Y. Harinath, Y. Suneetha, K. Seshaiah, A.V.R. Reddy, Synthesis, characterization, and biological activity of transition metal complexes of oxadiazole, Synth. React. Inorg., Met.-Org., Nano-Met. Chem. 41 (2011) 287–294.
[23] D. Grieshaber, R. MacKenzie, J. Voeroes, E. Reimhult, Electrochemical biosensors – sensor principles and architectures, Sensors 8 (2008) 1400–1458.
[24] A. Fatoni, A. Numnuam, P. Kanatharana, W. Limbut, P. Thavarungkul, A novel molecularly imprinted chitosan-acrylamide, graphene, ferrocene composite cryogel biosensor used to detect microalbumin, Analyst 139 (2014) 6160–6167.
[25] D. Udomsap, C. Branger, G. Culioli, P. Dollet, H. Brisset, A versatile electrochemical sensing receptor based on a molecularly imprinted polymer, Chem. Commun. 50 (2014) 7488–7491.
[26] M. Kyröläinen, S.M. Reddy, P.M. Vadgama, Blood compatibility and extended linearity of lactate enzyme electrode using poly(vinyl chloride) outer membranes, Anal. Chim. Acta 353 (1997) 281–289.
[27] S.M. Reddy, J.P. Jones, T.J. Lewis, Use of combined shear and pressure acoustic waves to study interfacial and bulk viscoelastic effects in aqueous polymeric gels and the influence of electrode potentials, Faraday Discuss. 107 (1997) 177–196.
[28] S.M. Reddy, G. Sette, Q. Phan, Electrochemical probing of selective haemoglobin binding in hydrogel-based molecularly imprinted polymers, Electrochim. Acta 56 (2011) 9203–9208.
[29] L. Bueno, H.F. El-Sharif, M.O. Salles, R.D. Boehm, R.J. Narayan, T.R.L.C. Paixão, S. M. Reddy, MIP-based electrochemical protein profiling, Sensors Actuat. B: Chem. 204 (2014) 88–95.
[30] S.M. Reddy, P.M. Vadgama, Ion exchanger modified PVC membranes-selectivity studies and response amplification of oxalate and lactate enzyme electrodes, Biosens. Bioelectron. 12 (1997) 1003–1012.
[31] Y.Q. Xia, T.Y. Guo, M.D. Song, B.H. Zhang, B.L. Zhang, Hemoglobin recognition by imprinting in semi-interpenetrating polymer network hydrogel based on polyacrylamide and chitosan, Biomacromolecules 6 (2005) 2601–2606.
[32] G. Vasapollo, R. Del Sole, L. Mergola, M.R. Lazzoi, A. Scardino, S. Scorrano, G. Mele, Molecularly imprinted polymers: present and future prospective, Int. J. Mol. Sci. 12 (2011) 5908–5945.
[33] S. Li, J. Wang, M. Zhao, Cupric ion enhanced molecular imprinting of bovine serum albumin in hydrogel, J. Sep. Sci. 32 (2009) 3359–3363.
[34] H.K. Yuen, E.P. Tam, J.W. Bulock, On the Glass-Transition of Polyacrylamide, in: J. Johnson, P. Gill (Eds.), Springer, US, 1984, pp. 13–24.